Exploring the formation of gold/silver nanalloys with gas-phase synthesis and machine-learning assisted simulations Supplementary information

Quentin Gromoff,[1] Patrizio Benzo,[1] Wissam A. Saidi,[2,3] Christopher M. Andolina,[2,3] Marie-José Casanove,[1] Teresa Hungria,[4] Sophie Barre,[1] Magali Benoit,[1] and Julien Lam[1,5,*]

[1] *CEMES, CNRS and Université de Toulouse, 29 rue Jeanne Marvig, 31055 Toulouse Cedex, France*
[2] *National Energy Technology Laboratory, United States Department of Energy, Pittsburgh, PA 15236, USA*
[3] *Department of Mechanical Engineering and Materials Science, University of Pittsburgh, Pittsburgh, PA 15261, USA*
[4] *Centre de MicroCaractérisation Raimond Castaing, Université de Toulouse, 3 rue Caroline Aigle, F-31400 Toulouse, France*
[5] *Univ. Lille, CNRS, INRA, ENSCL, UMR 8207, UMET, Unité Matériaux et Transformations, F 59000 Lille, France*

* julien.lam@cnrs.fr

A. EVALUATING THE ACCURACY OF A DEEP NEURAL NETWORK POTENTIAL (DNP) FOR AG-AU ALLOYS

In addition to Andolina et al.'s[**?**] validation tests, we tested the potential on three bulk alloys: $Au_{0.25}Ag_{0.75}$, $Au_{0.5}Ag_{0.5}$ and $Au_{0.75}Ag_{0.25}$. We evaluated bulk and surface properties. Our results show errors less than 1% for structural properties, and less than to 20% for mechanical properties and surface formation energies (Fig. 1) which are much more challenging to compute with accuracy.

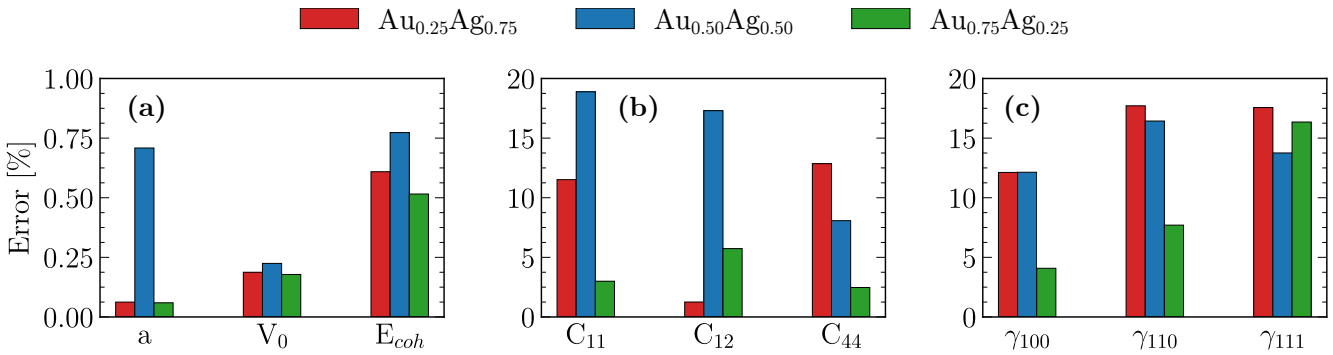

FIG. 1. (a) Lattice constant a, lattice volume per atom V_0 and cohesive energy E_{coh}. (b) Elastic constants C_{11}, C_{12}, and C_{44}. (c) Surface formation energies for (100), (110), and (111) surfaces.

Secondly, we tested amorphous structures. For this purpose, we applied the following procedure:

1. MD simulations were performed at 2000 K on supercells of $Au_{0.25}Ag_{0.75}$, $Au_{0.5}Ag_{0.5}$, and $Au_{0.75}Ag_{0.25}$ ordered alloys.
2. Ten snapshots were selected from the 2000 K MD trajectories to compute the forces using DFT.
3. The liquid structures obtained from the MD simulations were relaxed at 0K using the DNP.
4. After step 3, each structure was further relaxed using DFT.

The resulting changes after the final DFT relaxation are illustrated by the example shown in Fig. 2.

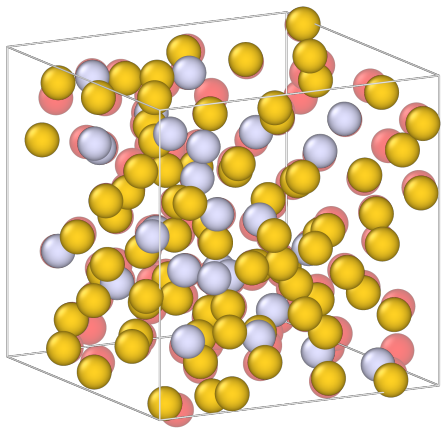

FIG. 2. Snapshot of a 108 atoms $Au_{0.75}Ag_{0.25}$ system after the quench and relaxation with DFT. Yellow (Au) and grey (Ag) atoms correspond to the structure after step 3. Red atoms correspond to the structure after step 4.

In Figure 3(a), the atomic displacements after the DFT relaxation (step 4) are presented: they show a tight distribution with a peak at 0.1 Å and an average displacement of MSD = 0.6 Å, demonstrating the validity of the DNP for disordered structures. In Figure 3(b), the comparison of the forces extracted from the liquid trajectories

and computed using the DNP and DFT are shown: we observe a sharp $y = x$ distribution, with no outliers. The root mean square error (RMSE = 0.07 eV/Å) is within the typical range for machine learning interatomic potentials in the literature.[**?**]

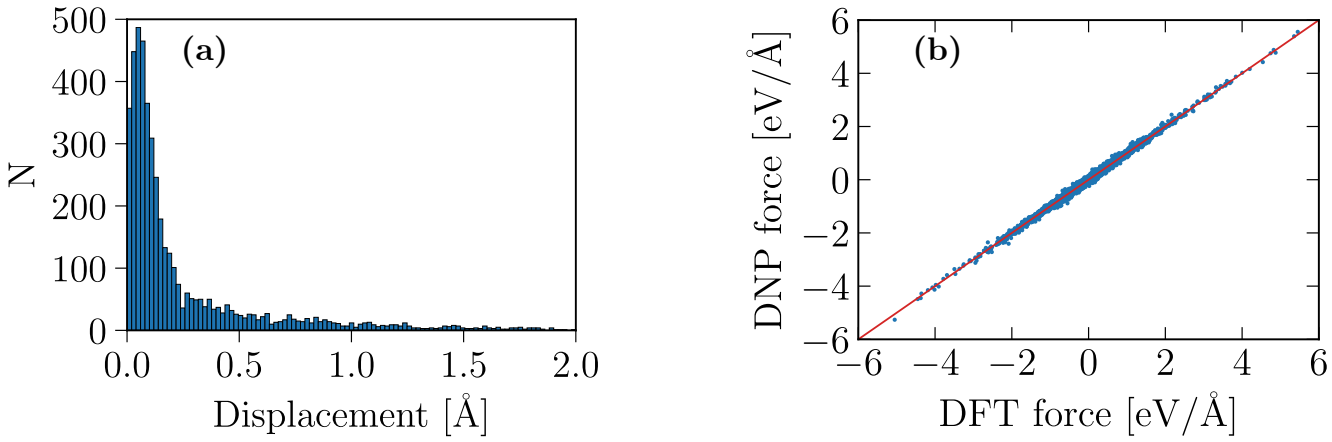

FIG. 3. (a) Distribution of the displacement of atoms between step 3 and step 4 of the procedure. (b) Distribution of the MD versus DFT forces from step 2.

B. HAADF-STEM OBSERVATION

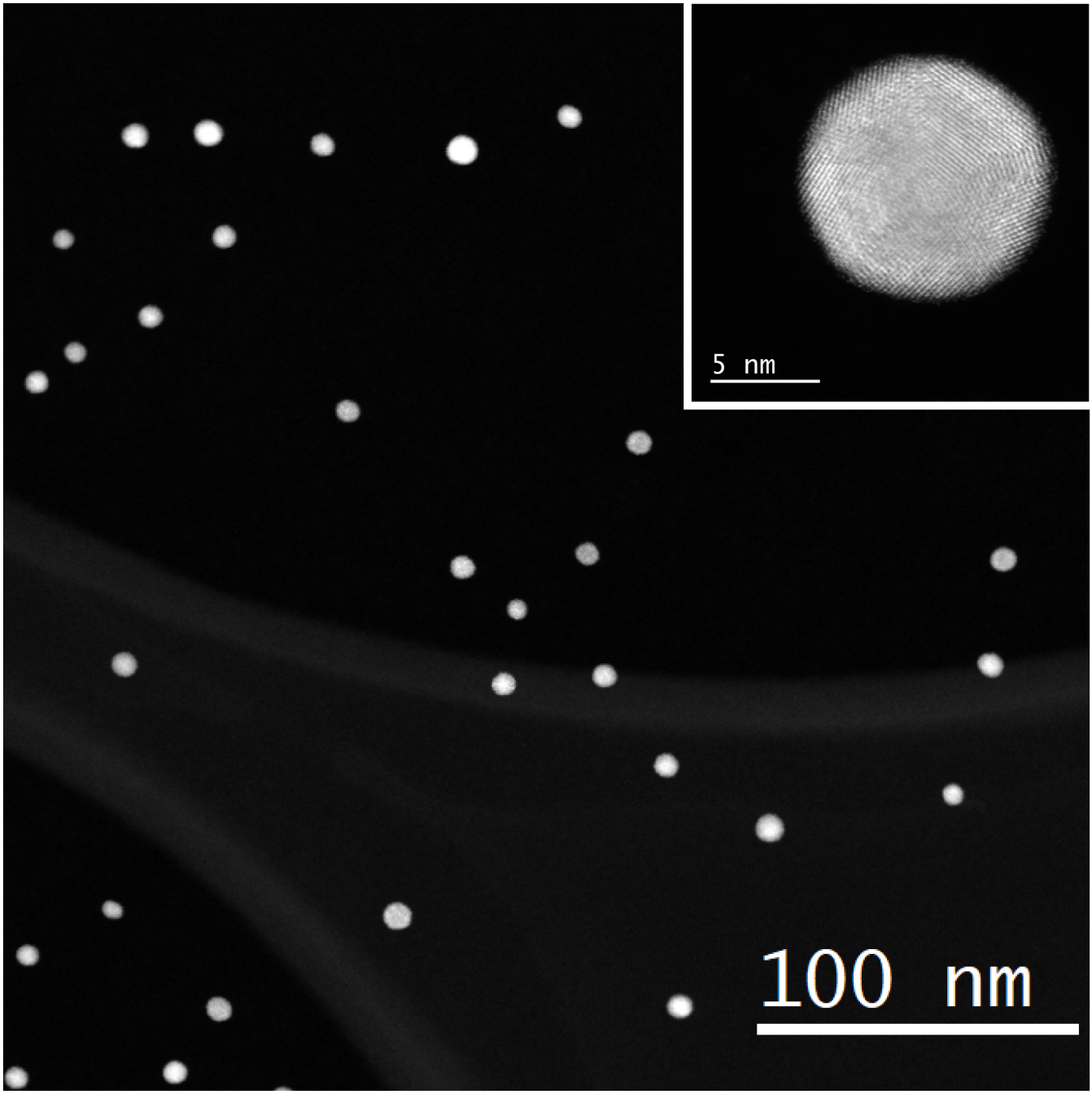

FIG. 4. HAADF-STEM observations of the AuAg nanoparticles synthesized by gas-aggregation magnetron-sputter deposition. The image in inset qualitatively reveal the gold surface segregation in a single nanoparticle (z-contrast).

C. RESULTS OF MONTE-CARLO AND ATOMIC SPECIES SWAPPING SIMULATIONS

Monte-Carlo (MC) simulations were conducted on nanoparticles obtained from MD freezing simulations using LAMMPS. The simulations were run for 300 ps while maintaining a constant temperature of 300 K. Additionally, an atom swap operation was performed on all atoms every 100 steps, with a maximum of 10 swaps per atom being allowed. As mentioned in the paper, the shape of the nanoparticles remained stable during MC simulations [see Figure 5], but a small change occurred in the ξ_{surf} as shown in Figure 6. It rose at the beginning of the run, then quickly reached a plateau, for all systems. This suggests a slight increase in gold segregation at the surface of the nanoalloys resulting from the atom swap mechanism. These MC simulations demonstrate that the gold segregation observed at the end of the freezing MD simulations is indeed a stable structure.

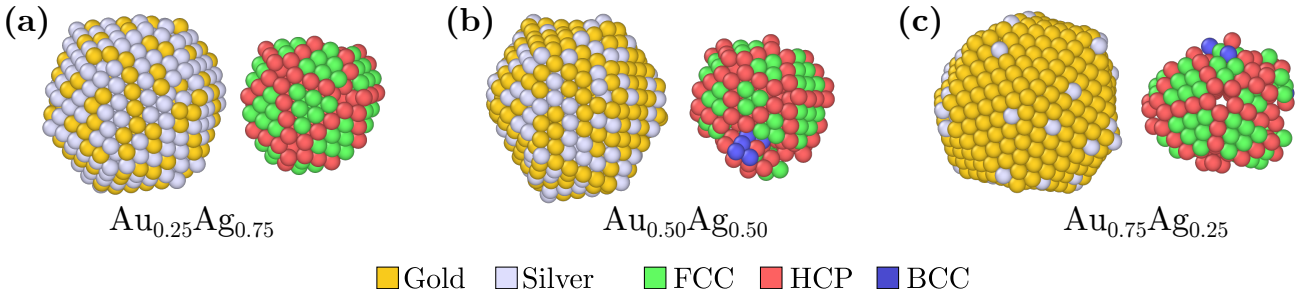

FIG. 5. Simulated nanoparticles from Figure 1 of the paper after MC simulations.

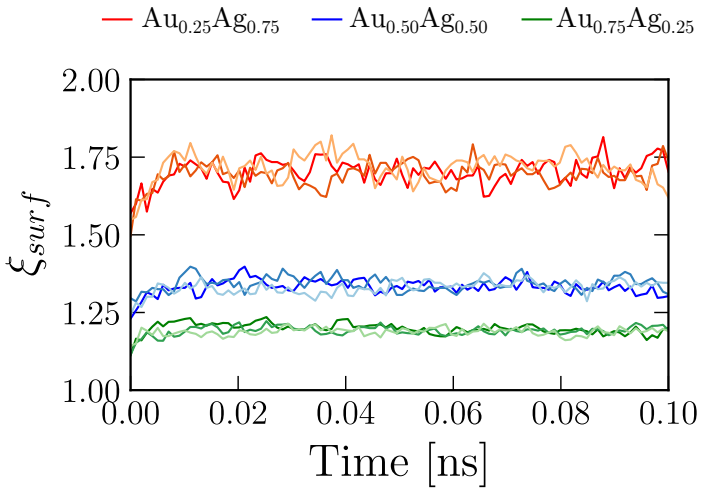

FIG. 6. Evolution of ξ_{surf} in 750 atom nanoparticles over the course of the MC run.

D. DENSITY PROFILE OF SIMULATED NANOPARTICLES

The goal of this section was to extract from the simulated nanoparticles a similar information as obtained by EDX measurements in the experiments. For this purpose, we plotted the distribution of the atoms as a function of the distance to the center of mass of the system for both chemical species. We note that with this approach, the integration volume decreases when r decreases which explains that the distribution tends towards 0 for small values of r. Despite lacking the clarity of the EDX profiles, it is still possible to compare the distributions of gold and silver in all systems. In particular, the gold segregation is clearly visible through the large peak which correspond to the surface layer.

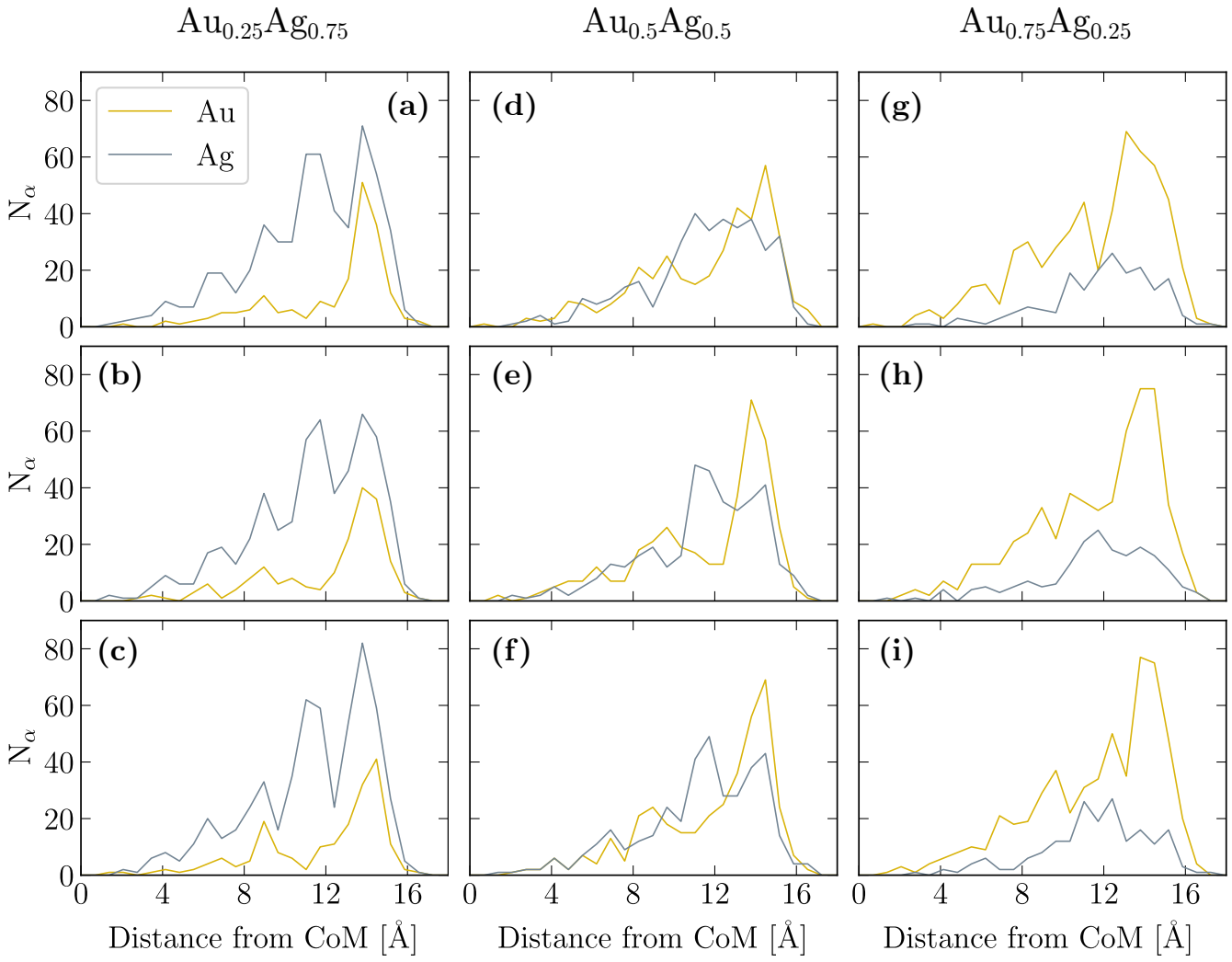

FIG. 7. Distribution of atomic species as a function of distance from the center of mass of the system. The NPs contain 750 atoms, (a,b,c) for $Ag_{0.75}Au_{0.25}$ systems, (d,e,f) for $Ag_{0.50}Au_{0.50}$ systems, (g,h,i) for $Ag_{0.25}Au_{0.75}$ systems.

E. STRAIN DISTRIBUTION

By comparing the structures obtained at the end of the freezing simulations with bulk structures, we managed to measure the strain distributions.

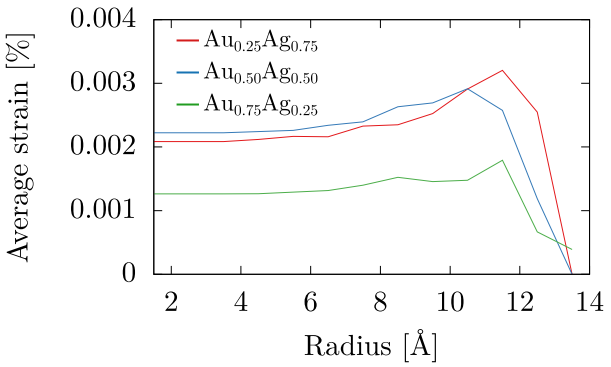

FIG. 8. Strain distribution averaged over the three different initial conditions for each chemical compositions and the nanoparticles of size 750 atoms.

F. MEAN SQUARE DISPLACEMENTS

Mean square displacement was measured as a function of the time. Then, results are averaged for atoms in the core and the surface of the droplet and over all of the initial conditions.

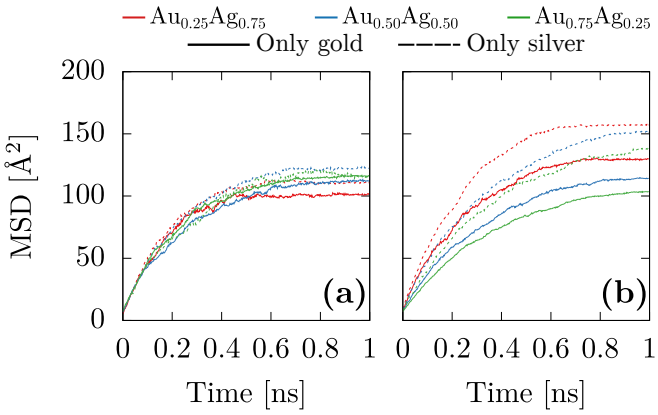

FIG. 9. Temporal evolution of the mean square displacement averaged over all of the initial conditions and measured for each chemical compositions and the 750 atoms nanoparticles. (a) and (b) represent respectively the core and the surface atoms.

G. ADDITIONAL TEMPORAL EVOLUTION OF SIMULATED NANOPARTICLES

Each MD simulation was run three times with different initial conditions. In Fig. 10, we collected the data from all of the 750-atom systems. The trends shown in Fig. 3 of the paper are still valid for the additional simulations. With the exception of one $Au_{0.5}Ag_{0.5}$ particle, the most gold-rich nanoalloys tend to have a low crystalline fraction. In order to make Fig. 10(c) more readable, we have not plotted the data for clusters of less than 50 atoms.

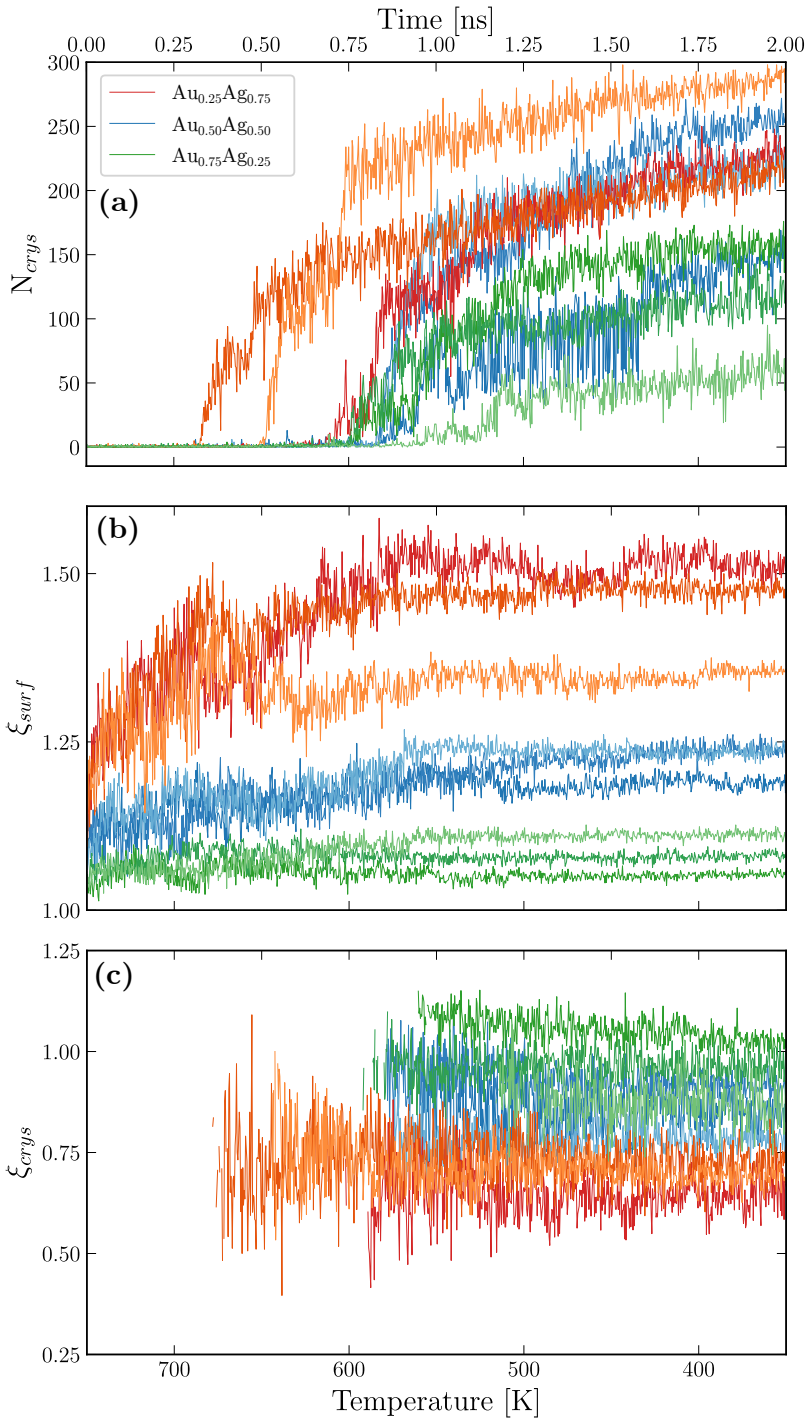

FIG. 10. Additional temporal evolution of N_{crys}, ξ_{surf}, and ξ_{crys} obtained in MD freezing with nanoparticles of 750 atoms. For each crystal, three runs were carried out with different initial conditions.

H. STUDY OF THE POSITION OF THE LARGEST CRYSTAL CLUSTER DURING MD SIMULATIONS

In Fig. 11, we show the evolution of the position of the largest crystal cluster at five specific sizes from 10 to 30 atoms. On the y-axis, we calculate the distance between the center of mass of the cluster and that of the whole nanoparticle, divided by the radius of the nanoparticle. Thus, a value greater than 0.5 shows that the cluster is located closer to the surface. Fig. 11(a), (b) and (c) show the results for systems with 250, 500 and 750 atoms, respectively. The most noticeable result is that crystallization begins near the surface of the droplet. We note that surface atoms cannot be classified as part of a crystal cluster due to the algorithm used, which explains why the cluster location can never reach a value of 1.

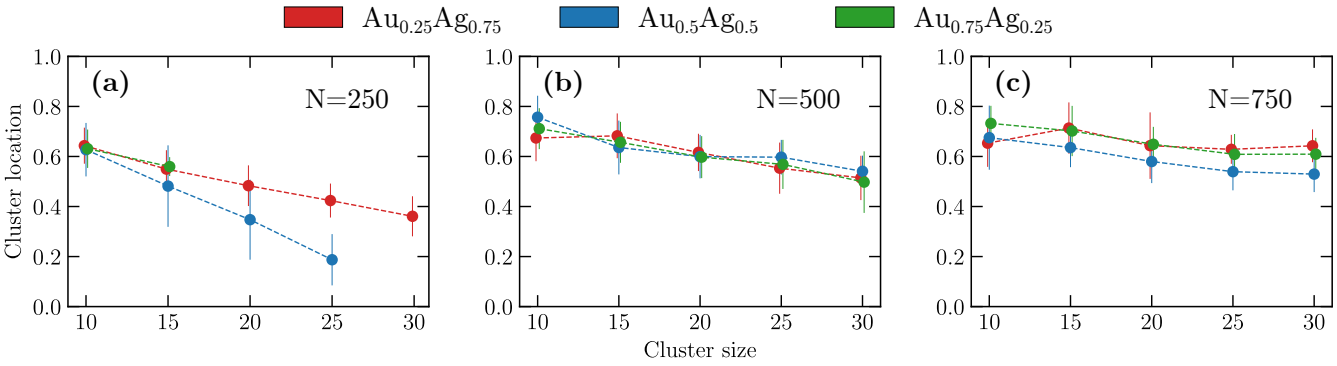

FIG. 11. Evolution of the position of the largest crystal cluster during the MD simulation for three different system sizes.

I. COORDINATION ANALYSIS OF SIMULATED NANOPARTICLES

Each column in Fig. 12 represents the evolution of the radial distribution function (RDF) for a 750-atom system throughout the freezing simulation. The combined partial distributions are consistent with a solid solution that the Au-Ag alloy is known to form. The transformation from a disordered structure to a more ordered structure can be seen by the increase in the height of the first peak and the appearance of additional secondary peaks at $t = 1\,\text{ns}$ and $t = 2\,\text{ns}$.

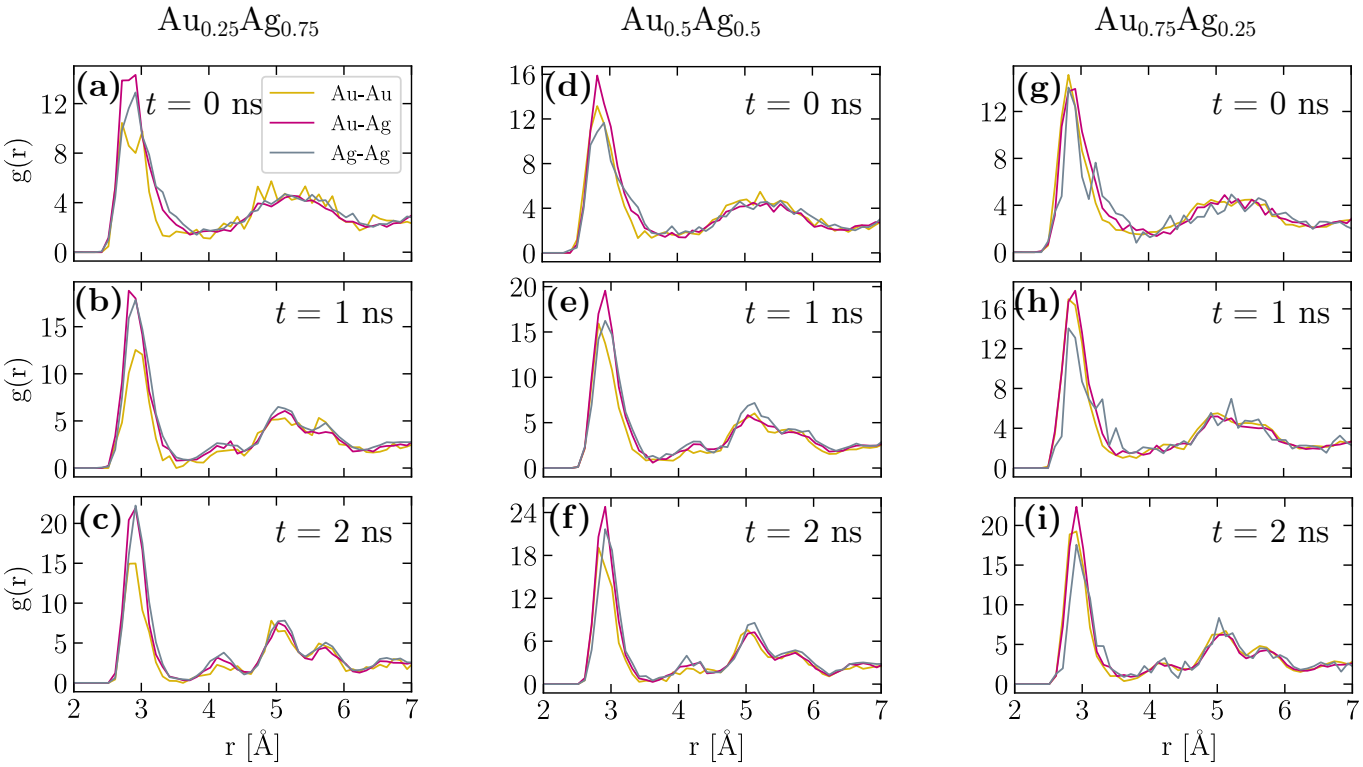

FIG. 12. Partial radial distribution functions RDF for three simulated 750-atoms NPs at different stages of the MD run.

J. RESULTS OBTAINED WITH EAM MODEL

We initialized calculations with nanoparticles made of 250 atoms that were obtained through machine-learning assisted freezing simulations and performed the same sequence of further stabilization that combine MD with MC moves and atomic species swapping at 300 K as described previously. Fig. 13.a shows that the nanoparticles obtained with the EAM model exhibit silver surface segregation. However, when performing DFT single point calculations, it appears that the nanoparticles are much more energetic than the gold segregated nanoparticles obtained with our DNP model [See Fig. 13.b].

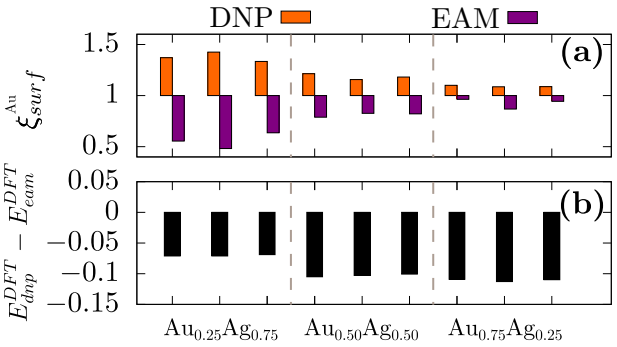

FIG. 13. (a) Value of the surface segregation for nanoparticles obtained with EAM and with DNP. (2) Energy difference between the corresponding nanoparticles.